SEGO RESOURCES INC.

MINER MOUNTAIN PROJECT

PRINCETON, BC

TITAN 24 RE PROCESSING

HELI MAGNETICS AND RADIOMETRICS

INTERPRETATION

COMTEK ENTERPRISES LTD.

Jules J. Lajoie
June, 2013

TABLE OF CONTENTS

TABLE OF CONTENTS 2
INTRODUCTION 3
TITAN 24 RE PROCESSING 3
Preamble 3
Processing Steps: 4
Processing Products: 5
Sample Comparison Using Line 685000E: 7
PRECISION GEOSURVEYS MAGNETICS AND RADIOMETRICS 9
Standard RMI map: 10
Reduced to Pole Map: 11
First Vertical Derivative Map: 12
Analytic Signal Map: 13
K-Th Ratio map 14
3D Inversion Model 15
EXPLORATION SIGNATURES 16
INTERPRETATION 17
1. Cuba Zone Extensions 18
2. Quintana Zone 18
3. Regal Zone 19
4. Southwest Zone 19
5. Southeast Zone 20
6. Deep East Zone 20
7. North Zone 22
8. North End Zone 23
CONCLUSIONS 24
REFERENCES 25

INTRODUCTION

This report addresses two geophysical datasets on the Miner Mountain property of Sego Resources Ltd., located immediately northeast of Princeton BC. These are:

1. 2009 Quantec Titan 24 Survey: The work on this dataset consisted of a complete reprocessing of the original field data because some of the inversion results did not appear geologically plausible.
2. 2013 Precision Geophysics Heliborne Aeromag and Radiometric Survey: The work on this dataset consisted of generation of new map products.

The results are then interpreted to generate exploration targets. Property description, geology, and exploration history are all available elsewhere and so this report is intended for a reader who is familiar with the property.

TITAN 24 RE PROCESSING

Preamble

Titan 24 is a distributed array Resistivity and Induced Polarization system. A long potential dipole (a=100M) array is laid out and data is collected simultaneously on all of them from a transmitter electrode that is located in the center of a dipole and then moves sequentially through the whole array. In essence, standard pole dipole left and pole dipole right array information is embedded in the data, with n spacings of n=0.5 up to about n=29.5. However, standard pseudosection data displays were not included, only inversion sections. Thus, if some of the inversions do not appear correct, there is no pseudosection to compare with for validation or checking.

The survey results are described in the Quantec report (Gharibi and Hearst, 2009). 13 N-S lines, near 3 kms long, were surveyed at 200M spacing in the center of the property from UTM eastings 682800E to 685200E. The Quantec report retained the last 5 significant figures of NAD 83 UTM coordinates. This system was retained for all section displays herein. However, derived horizontal grids and 3D voxels were converted to full UTM coordinates for correct georeferencing with other data.

The objective of the reprocessing was to attempt to achieve inversion results that are more geologically valid, that is having a less “blobby” appearance and with better line to line continuity than what was presented on some lines of the original inversions, this to be demonstrated later.

In this writer’s opinion, IP data for n spacings greater than about 12 are probably too noisy. Resistivity data are valid for n spacings greater than that, but their incremental exploration value is questionable. Furthermore, the higher the n spacing, the fewer the data points available for a constant array spread length.

Herein, Pole Dipole Left means the dipole is on the LEFT side, or SOUTH since line displays all look west in this survey. Pole Dipole Right is simply the opposite.

Processing Steps:

1. Start with Quantec archive spreadsheet files called Line#-final.csv.
2. Separation of the data into independent Pole Dipole LEFT (PDL) and Pole Dipole RIGHT (PDR) datasets for each line.
3. Delete n separations of 0.5, deemed to be hypersensitive for subsequent inversion work.
4. Delete n separations greater than n=11.5
5. Generate standard pseudosections of apparent resistivity and chargeability with data repeats averaged. Consistent color ranges are used.
6. Careful inspection of each pseudosection for data realizability, that is, removing data deemed to be unrealizable or too noisy, whether a repeat value or a single value at a station. Pseudosections are then regenerated and the process is repeated until results are satisfactory. In the end, this process removed a few percent of data. In this writer's opinion, the data is of excellent quality.
7. Inversion of the data using UBC 2D inversion codes, using more relaxed parameters than was likely previously used.
8. Inspection and comparison of the independent inversions from PDL and PDR for each line, to ensure reasonable compatibility. Those that were not, were re-edited and re- inverted until results were satisfactory. Remaining minor differences between PDL and PDR inversion results reflect the inherent uncertainty of geophysical inversion.
9. The inversion results were clipped at 500M depth from highest elevation on each line.
10. The inversions were then clipped in a N-S direction to reflect the range of valid information:
    PDL: 83200N to 85300N
    PDR: 83100N to 84800N
    As well, line 682800E is removed from the PDL products due to inversion difficulties experienced with this line. The area of influence of the two survey types is shown on various maps.
11. Stitching and gridding inversion results into 3D voxels with 10M cells for smooth presentation. Topography was used to clip off the top cells. The voxels are referenced to full UTM coordinates for correct georeferencing.
12. Generation of grids from the top cells of the voxel models to display the resistivity and chargeability at surface.

Processing Products:

1. All standard pseudosections with topography, as Geosoft Packed Maps and png images. Example:

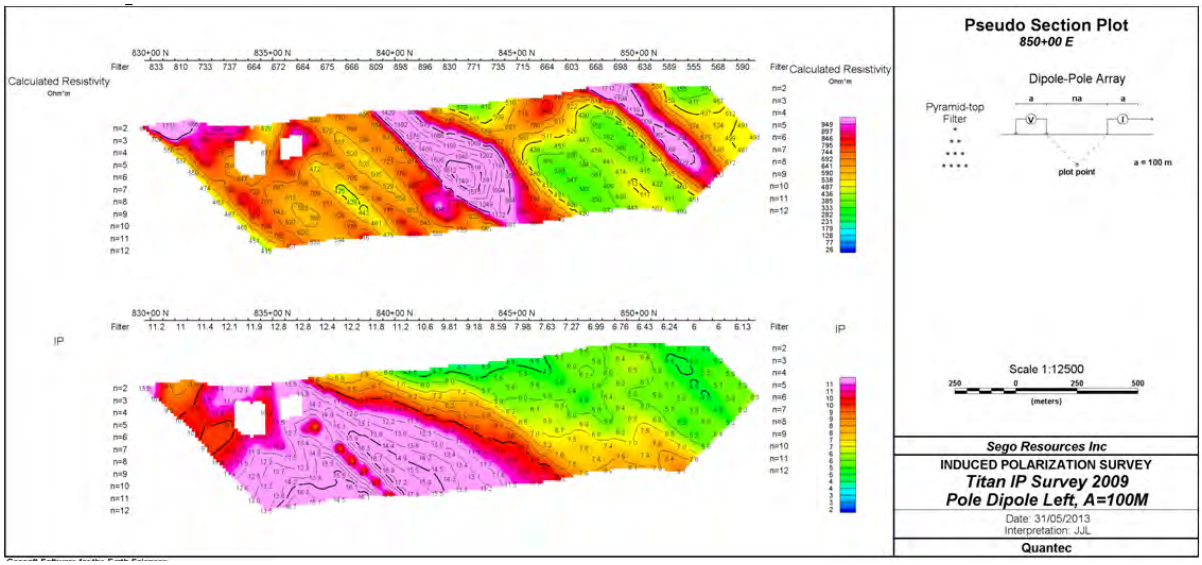

2. UBC inversion results as copies of UBC GUI images preserved in Word files, displaying inversion, convergence functions, and comparison of observed vs predicted data.

3.All inversion sections as Geosoft packed maps and png images. Example:

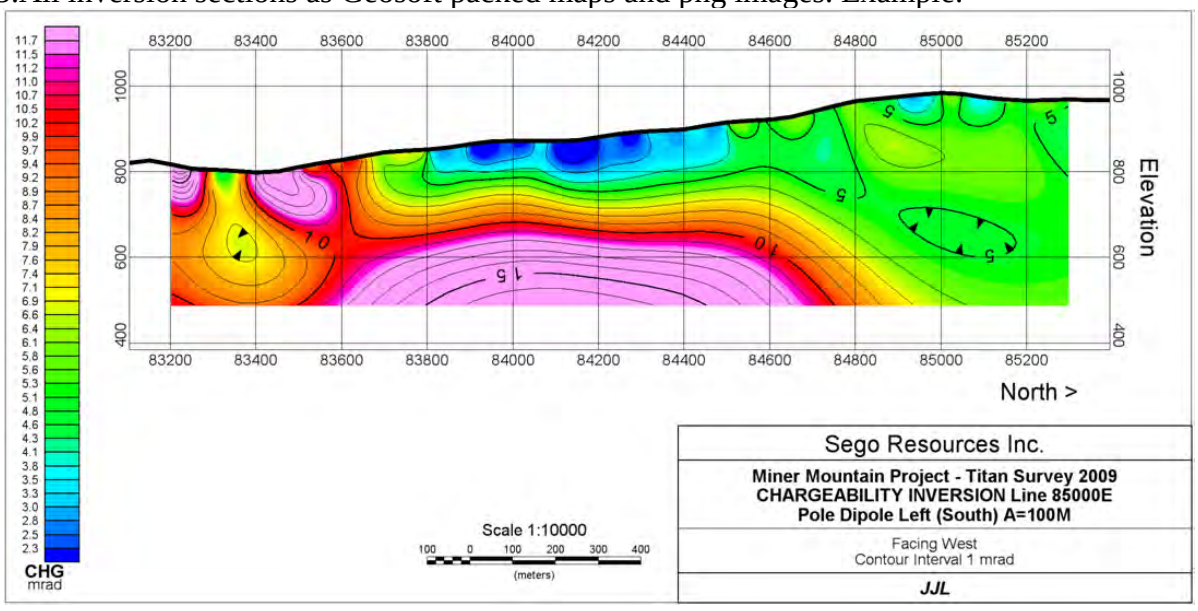

4. Digital Voxel models for PDL and PDR resistivity and chargeability, that can be viewed, sliced, and clipped in a number of applications. Example below is a N-S slice of the 3D PDL topography clipped chargeability inversion through Cuba and Quintana zones, looking NW, demonstrating the smooth character of the model.

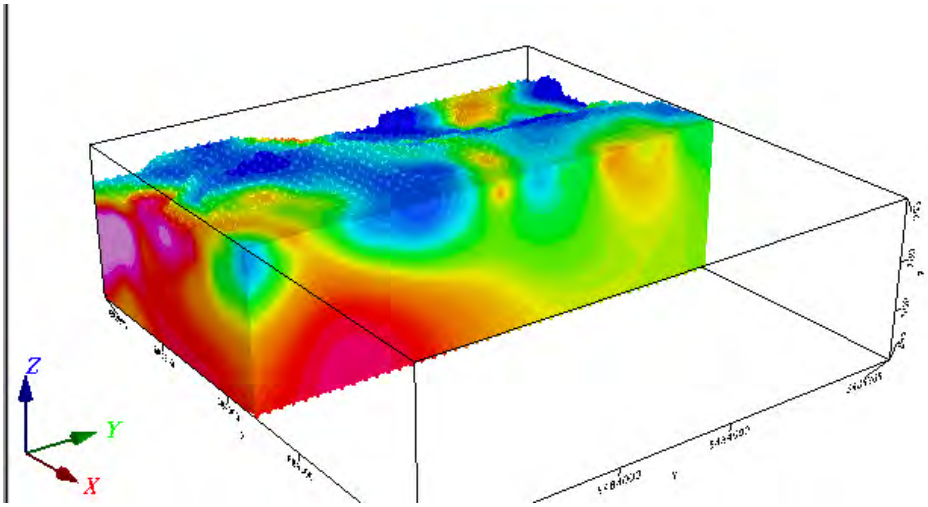

5. Grids generated from voxel top cells to display data on the topography surface. Example for PDL chargeability, displaying smooth data character from line to line:

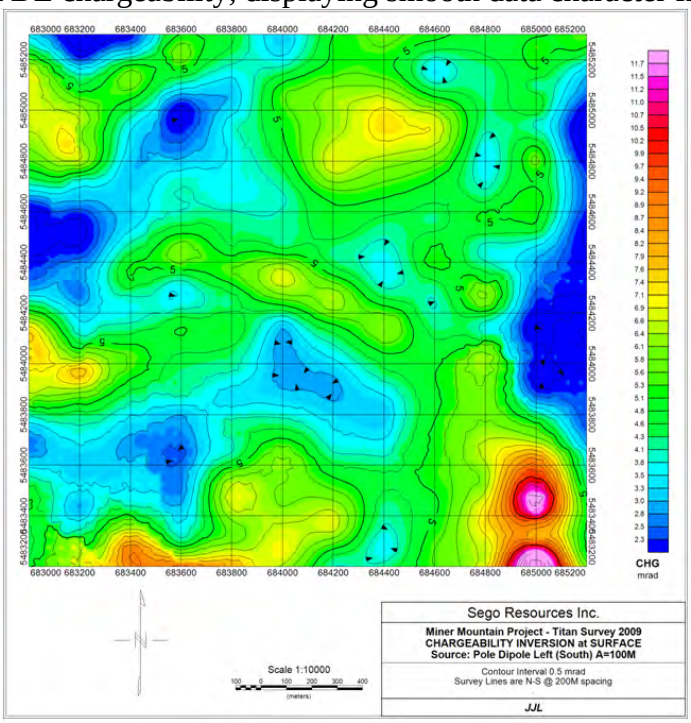

Sample Comparison Using Line 685000E:

The following figure shows Quantec Chargeability Inversion for Line 85000E (Fig 16 in Quantec report) with target numbers identified:

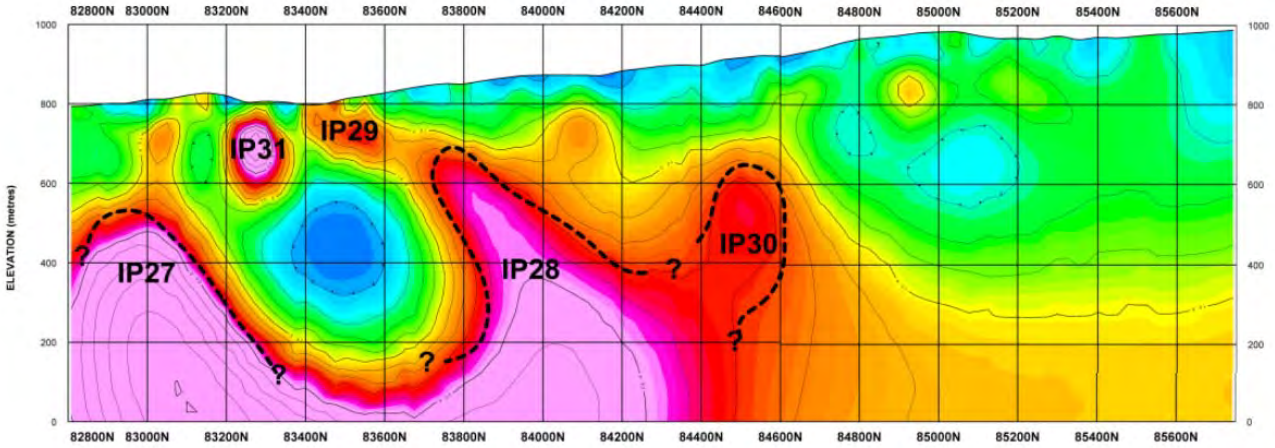

The Quantec report did not display standard pseudosections. The work herein included the generation of standard pole dipole left (PDL) and pole dipole right (PDR) pseudosections as the basis for quality control and editing.

Following is the Pole Dipole Left edited Pseudosection data extracted from the digital data:

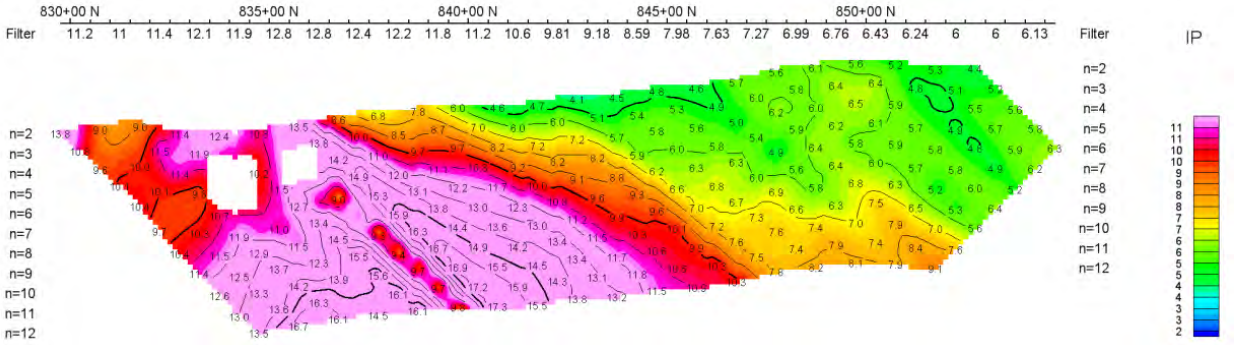

Following is the Pole Dipole Right edited Pseudosection data extracted from the digital data:

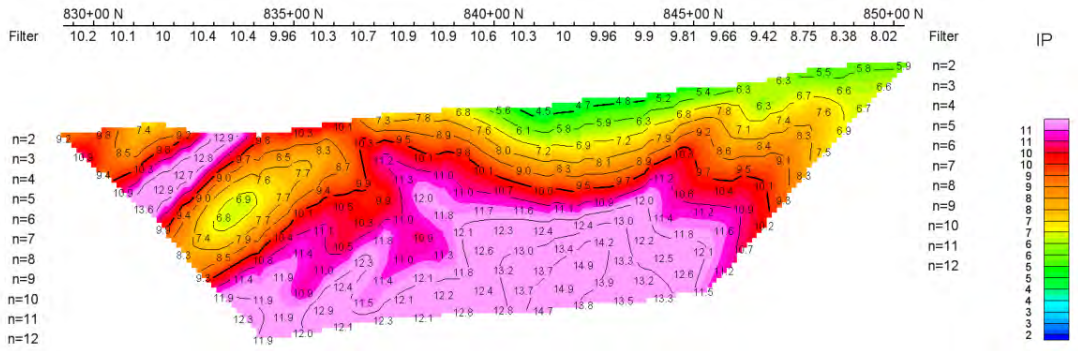

The derived pseudosections are compatible with each other. An experienced pseudosection interpreter would interpret a shallow source in the vicinity of 835+00N and a significantly larger deeper source centered at about 840+00N. In the opinion of this writer, these pseudosections do not support the complex Titan inversion model shown at the top, which appears to result from over fitting the data, a common problem in geophysical inversion.

Following is the Comtek Pole Dipole Left Chargeability Inversion for Line 85000

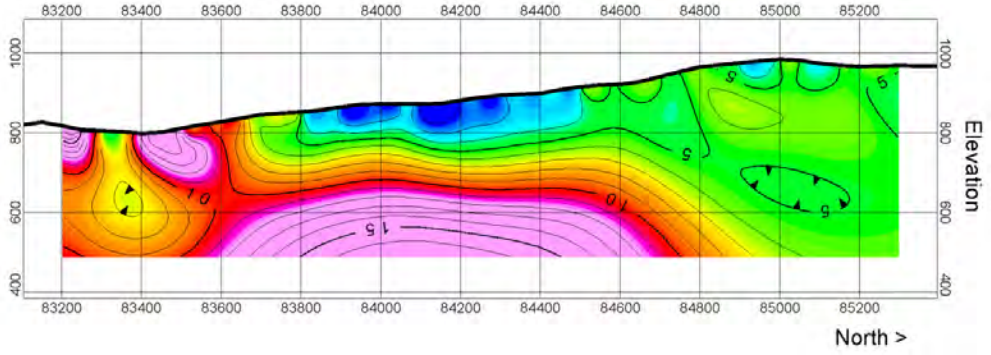

Following is the Comtek Pole Dipole Right Chargeability Inversion for Line 85000

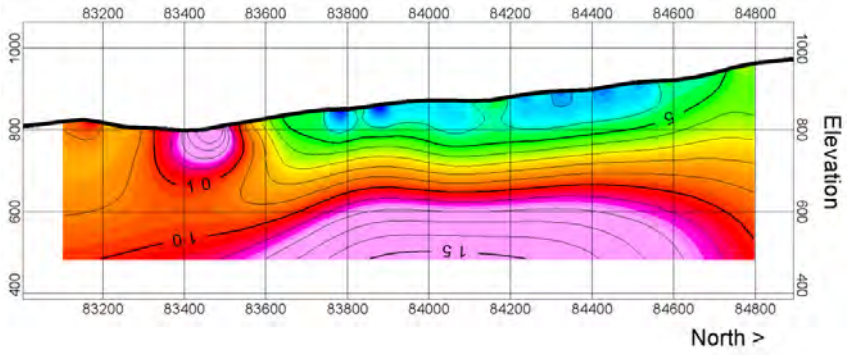

The above two independent inversions are in good agreement with each other and a better explanation of the pseudosection data. The southernmost chargeability high at 83200N at the south end of the PDL inversion is admittedly unreliable, being at the extreme end of the line. However, as seen on both independent inversions, there is a clear shallow source at 83450N and a broader deeper source from 83600N to 84600N, keeping in mind that the latter could be off line.

This demonstrates the smoother more geologically plausible inversions produced herein. They then contribute to much better 3D voxel models and surface (top cells) maps as demonstrated in the displays of the previous section.

The collected data is considered to be of excellent quality. Nevertheless, all surveys have some bad data. It's normal. In this work, the PDL data for the westernmost line 682800E was causing a lot of difficulty in inversion and was finally abandoned. This is of no real consequence because much of this line is on the western side of the Boundary fault, and the southern end of that line near the Southern mineralized zone is well covered by the PDR data which extend further south anyways.

PRECISION GEOSURVEYS MAGNETICS AND RADIOMETRICS

The Miner Mountain property was surveyed in 2013 by helicopter borne magnetics and radiometrics on N-S lines 100M apart with fill in lines at 50M spacing in the south central area of drilling. The results and excellent survey products are described in the Precision GeoSurveys Report (Poon, 2013) and need not be repeated here. A total of 288 line kms were surveyed. There is a small gap in the data south of the Cuba zone, due to a microwave tower.

Herein, additional map products are generated and of course the results are used in the interpretation.

Property wide map products produced herein and called Main--, do not include the infill lines because very slight errors caused by things like elevation differences can result in troublesome gridding issues in derivative products. Addition of the infill lines does not significantly change the picture, outside of reducing the footprint of some single line anomalies simply because they would be gridded over 50M to the next line rather than 100M.

A separate set of maps was generated for the infill area, called Infill--, wherein all in fill lines were included. This infill datasets was used to generate the 3D magnetic inversion model.

All map products are available digitally as Geosoft maps and png images. Some of the maps additional to those generated by Precision are shown in the following pages with accompanying descriptions. There is as well a composite map in the digital files containing all the different geophysical product layers, along with other registered layers of geology, geochem, etc.

Following pages show basic new maps for the main area, without the infill lines, along with comments. The PDL and PDR outlines on the maps show the areas of influence of the PDL and PDR 3D IP inversion models.

Standard RMI map:

Following is the map of Residual Magnetic Intensity (RMI) derived by subtracting the International Geophysical Reference Field from the observed Total Magnetic Intensity (TMI):

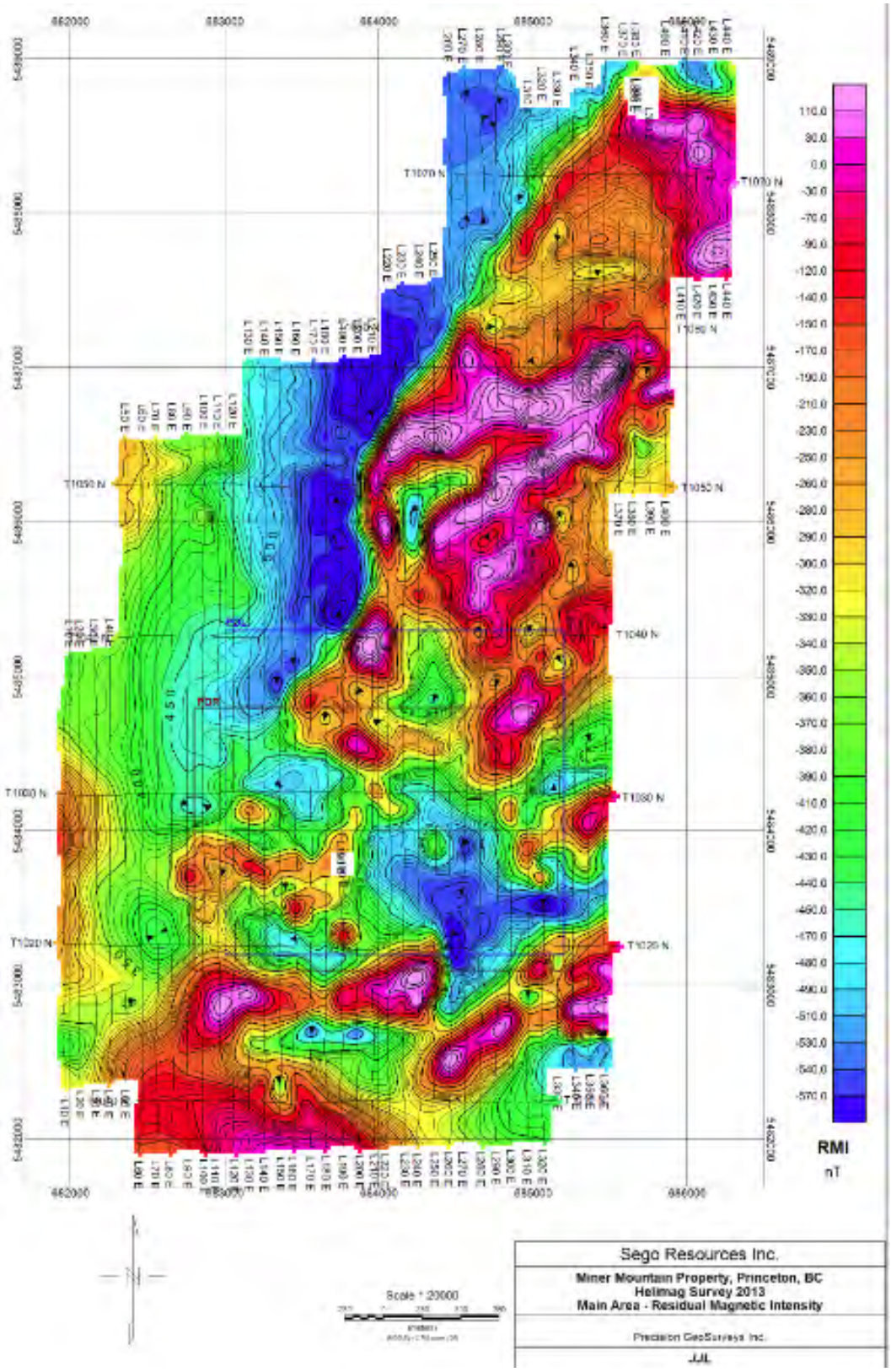

Reduced to Pole Map:

Following is the Reduced to Pole map (RTP). Anomalies are seen to shift a bit north by a distance which is a function of anomaly wavelength.

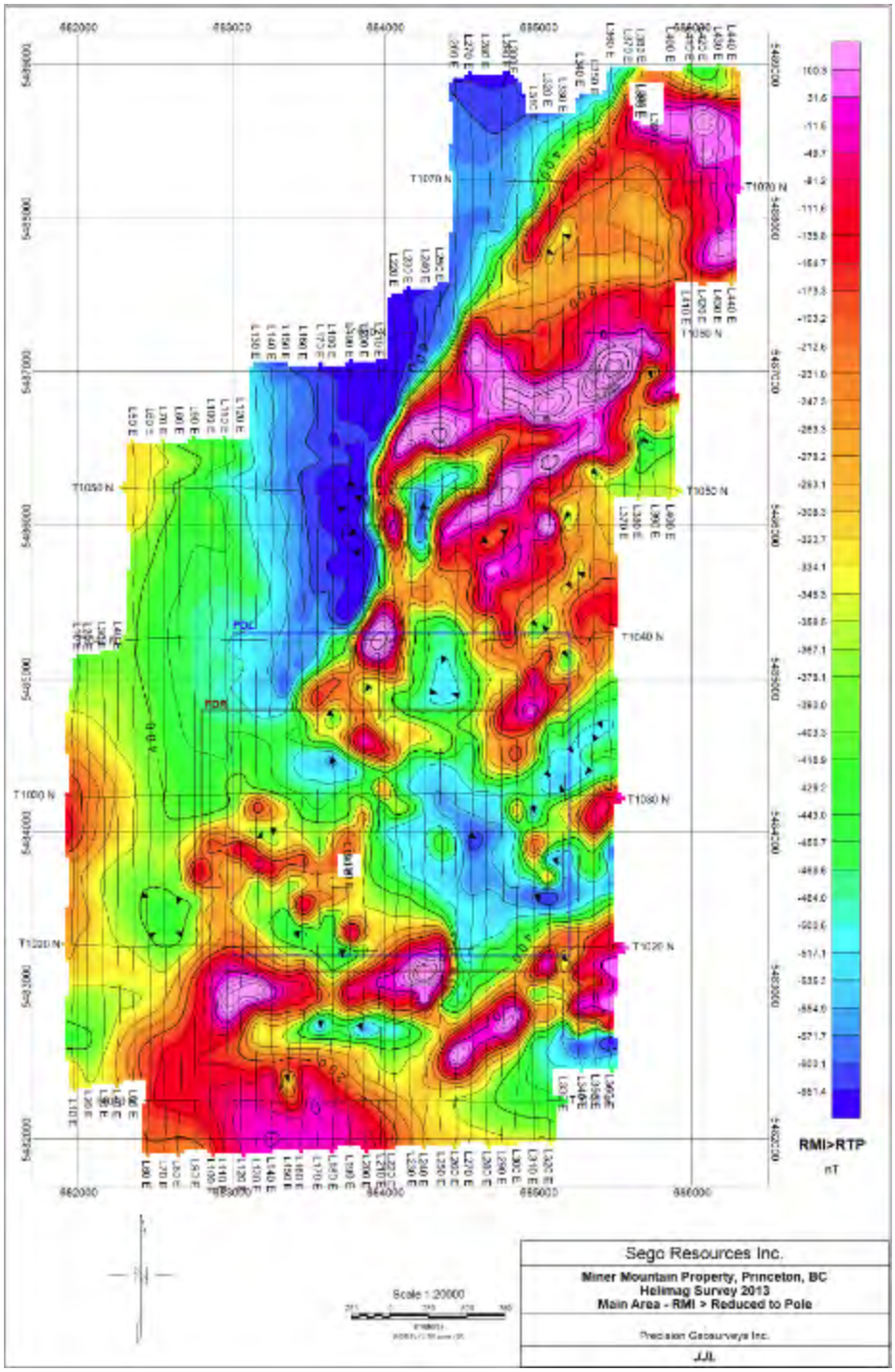

First Vertical Derivative Map:

Following is the first vertical derivative map(1VD), derived from the RTP map. It clearly focuses attention on the high frequency content in the data.

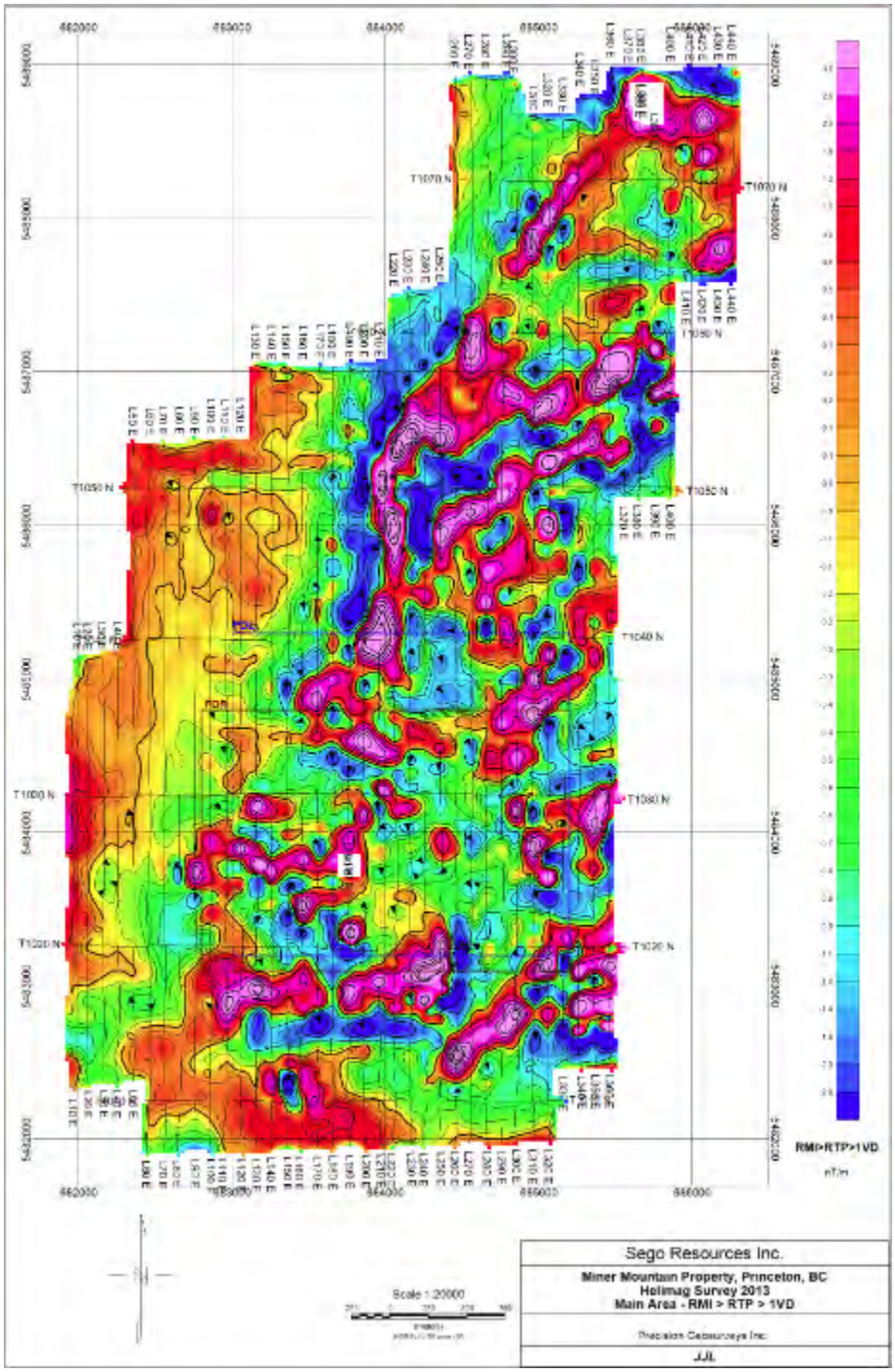

Analytic Signal Map:

Following is the analytic signal (AS) map, computed from the RTP map. Analytic signal is just the square root of the sum of squares of all three directional derivatives. It has a high pass or high frequency look to it, like that of the 1VD, but with two major differences. The first desirable AS property is that the result is almost invariant to magnetization direction. Secondly, it responds to magnetization intensity. The latter means that a reversely magnetized body due to remanent magnetization that produces a negative anomaly in TMI or 1VD maps, will instead produce a positive anomaly in the AS map. A perfect example of this can be seen in the sharp single line negative anomaly near the south end of airborne line 150E, just north of the tie line. It is clearly negative in both RMI and 1VD maps. However, the AS map produces a positive at this location.

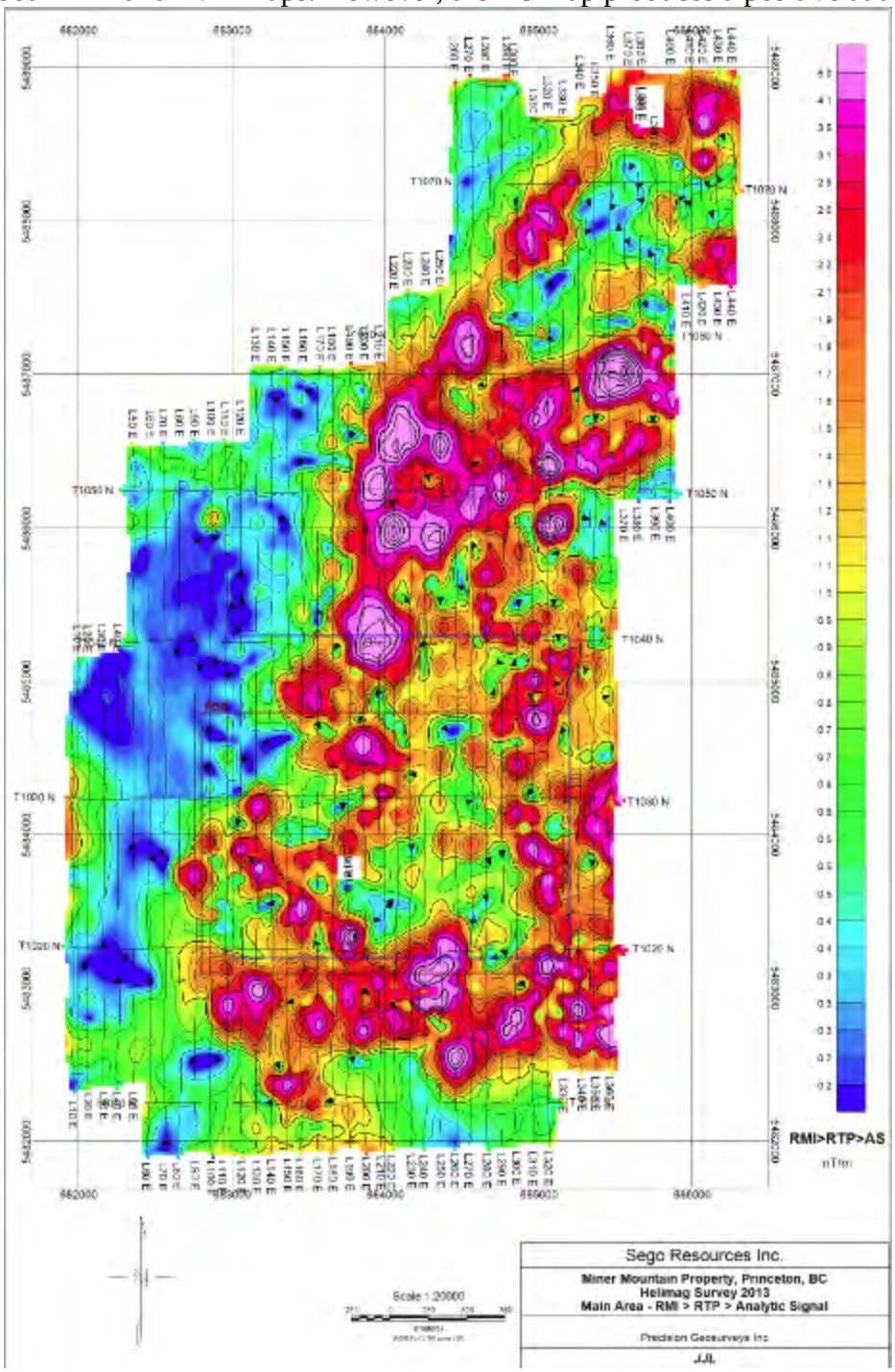

K-Th Ratio map

Most airborne contractors generate maps of Thorium to Potassium ratios. This requires searching lows for areas of potassium alteration highs. Herein, this number is simply inverted to K/Th ratio such that the desirable K highs produce highs (reds) on maps, as this is easier for the eye to focus on. Below is this map:

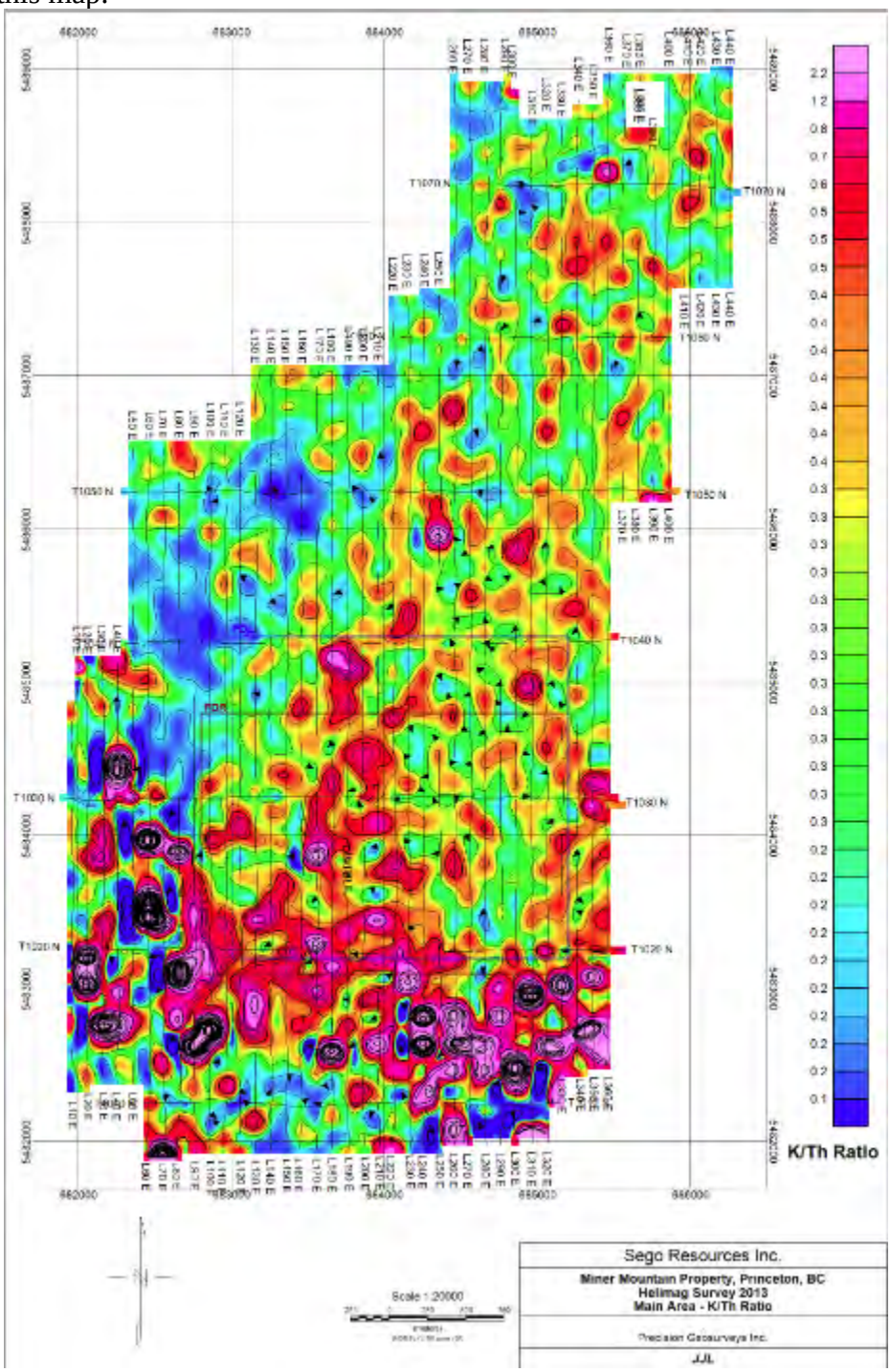

3D Inversion Model

To obtain a 3D magnetic inversion model of the infill area, the in fill data were expanded by about 500M using the 100M spaced data for adequate surrounding padding. The residual magnetic intensity (RMI) data were used after adding a constant of 700nT for positivity. Thus the data and 3D model represents anomalous susceptibility.

After a number of iterations using improving inversion parameters, a 3D inversion model with 10M cells was finally produced for the central area of infill lines of about 2.4 kms square. The limits for the model are:
X 682850E to 685200E
Y 5482800N to 5485200N
Z 400M elevation and above.

Being a fundamental limitation of the non uniqueness of depth in magnetic and gravity data, the 3D model should not be relied on in detail for depth information. This situation is better for IP type of data because the multiple separations provide depth control.

Below is a view of the 3D susceptibility inversion model looking NW and clipped N-S at 684400E near the center.

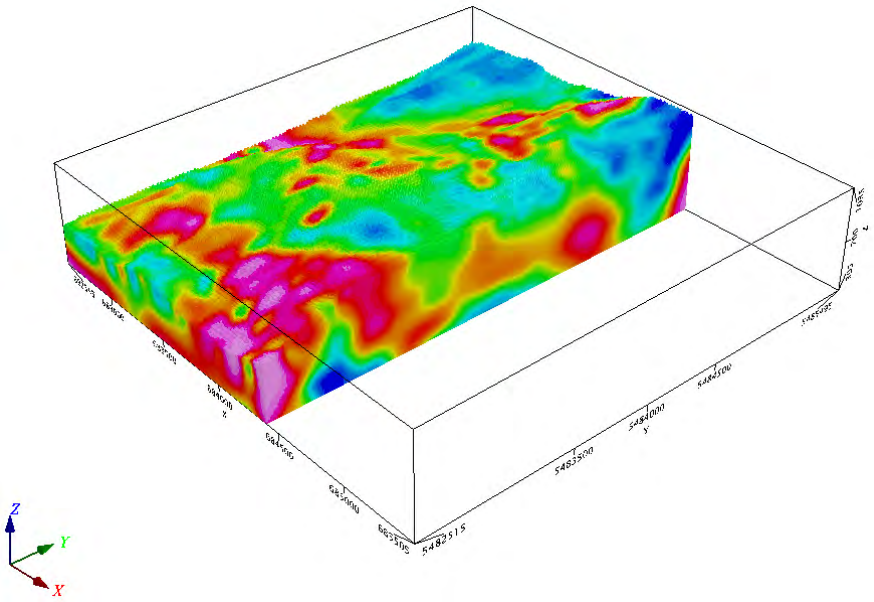

EXPLORATION SIGNATURES

A review of the literature on the Copper Mountain Mine about 25kms to the south (i.e. Stanley et al., 1995) highlights a number of usefull exploration characteristics. The first is proximity to the Boundary fault, part of a major N-S structural corridor, a crustal zone of weakness for mineral generating intrusions. A number of mineral occurrences are proximal to this corridor further north. The Miner Mountain property is well located in this regard. The Copper Mountain deposits exhibit clustering, a characteristic of alkaline Cu-Au deposits. The Copper Mountain deposits are located on the edges of strong magnetic anomalies that are related to intrusive bodies which can produce magnetic highs or lows depending on magnetite preservation or destruction. One of these is the Lost Horse Intrusive Complex, one phase of which is interpreted to be directly related to mineralization. Available mag information does not display a direct mag correlation with the deposits but it possible that such would be displayed in a high resolution survey as was done at Miner Mountain. The deposits are associated with high carbon and low pyrite suggesting that IP anomaly amplitudes will be subdued. The Copper Mountain deposits are nevertheless known to be associated with IP anomalies.

On the Miner Mountain property, there is an excellent correlation of the Cuba zone mineralization with a weak, 2-3 mrad, yet distinct IP response. The following figure shows the surface cells of the 3D PDL chargeability inversion model. The squares are 1 km. The white outline shows the Cuba zone drilling.

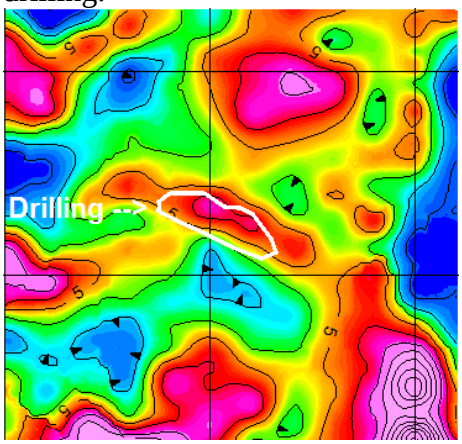

This next figure shows approximately the same area on RTP background showing that the Cuba zone is associated with a WNW trending magnetic low which appears to be an arm extending out from a strong mag low located about 500M to the SE. The mag low trend appears to be transected by a NNE trending mag high.

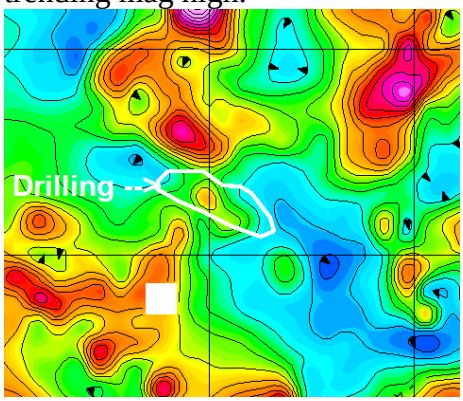

The Cuba zone does not have an obvious correlation with K/Th ratio.

INTERPRETATION

The following figure shows a shaded RTP map on which a number of faults are interpreted. In particular, the Boundary fault displays a prominent magnetic break striking NE across the whole map with a clear offset about 2 kms north of the Cuba zone. The indicated faults are only preliminary interpretation made without in depth knowledge of the property geology. The point is that this dataset and other products derived herein should be used continually to aid geologic interpretation as new information becomes available. Varying shading direction is particularly helpful. The map displays numerous magnetic anomalies, highs and lows, and along with strong evidence of structural disturbance (faulting), it shows a setting permissive for multiple intrusions and clustering of alkalic Cu-Au deposits.

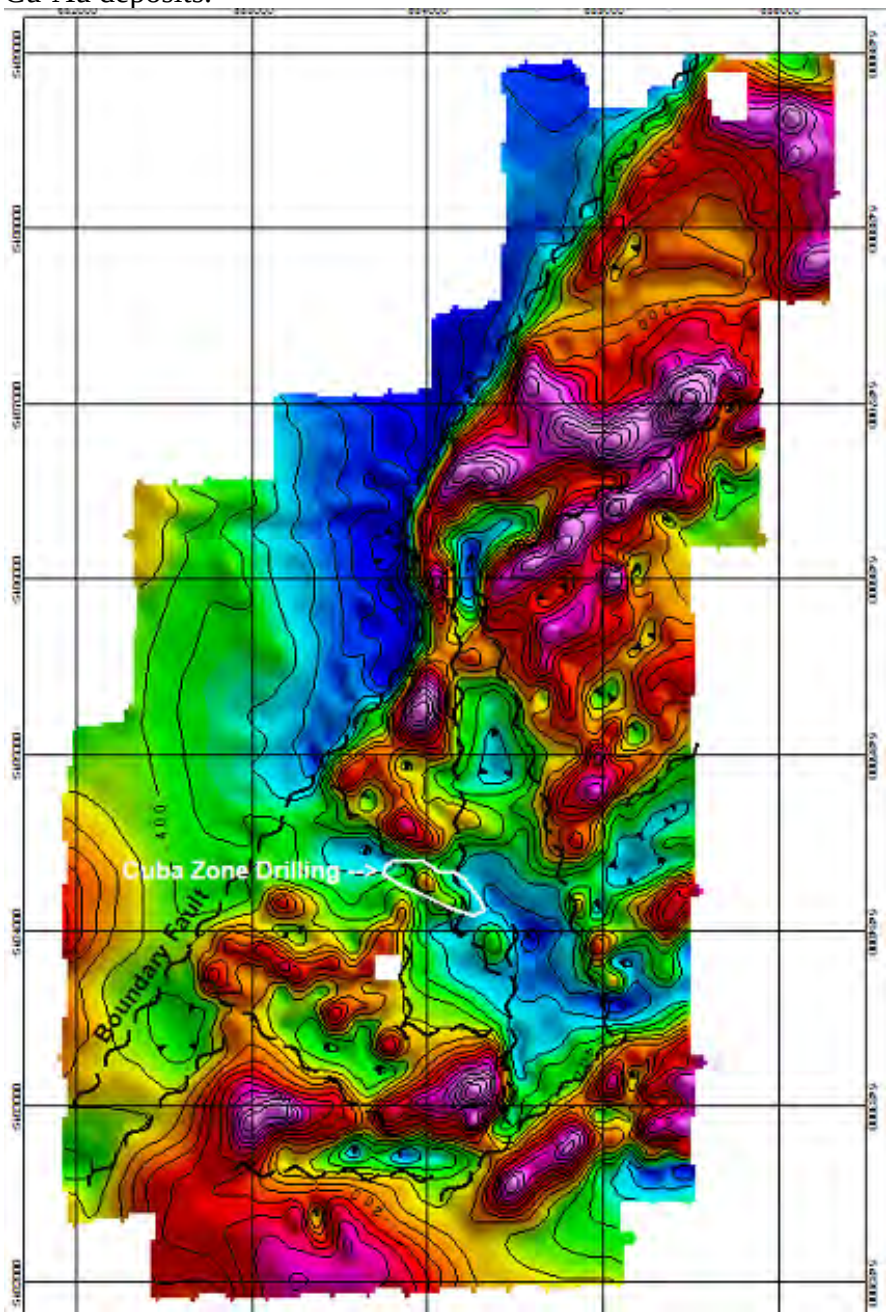

The following outlines a number of target areas interpreted from the datasets herein. Grid lines within the images are 1 km. The first set of six consists of targets supported by IP data.

1. Cuba Zone Extensions

The following figure of top cells of the 3D IP PDL model shows that the Cuba zone, as defined by percussion drilling, correlates well with a weak IP response that strongly suggests extension of the zone further to the WNW and ESE into local mag lows. These are obvious drill target areas. Furthermore, there is a suggestion in the 3D IP model that the zone plunges to depth to the ESE, into a strong deeper IP source described later, and through an interesting mag low area.

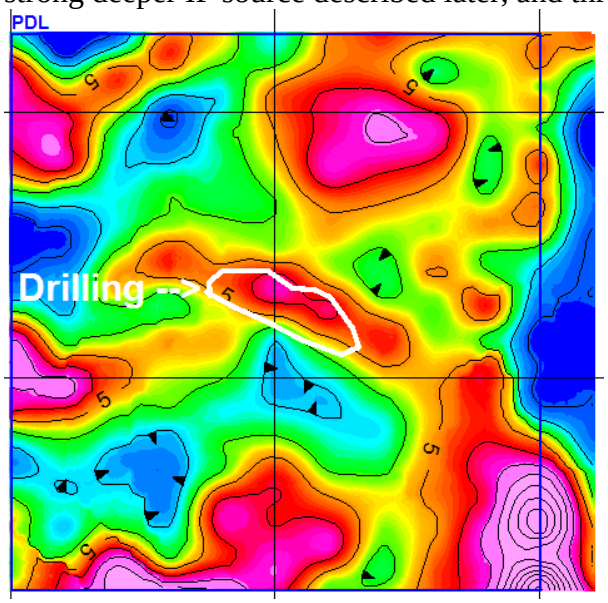

2. Quintana Zone

The untested Quintana zone is located about 700M NE of the Cuba zone. The following figure shows color IP with contours of RTP mag. A sub circular 500M diameter IP response (3D PDL model top cells) coincides with a mag low suggesting magnetite destruction. Drilling is recommended at 684400E, 5484950N to test the center of this combined response.

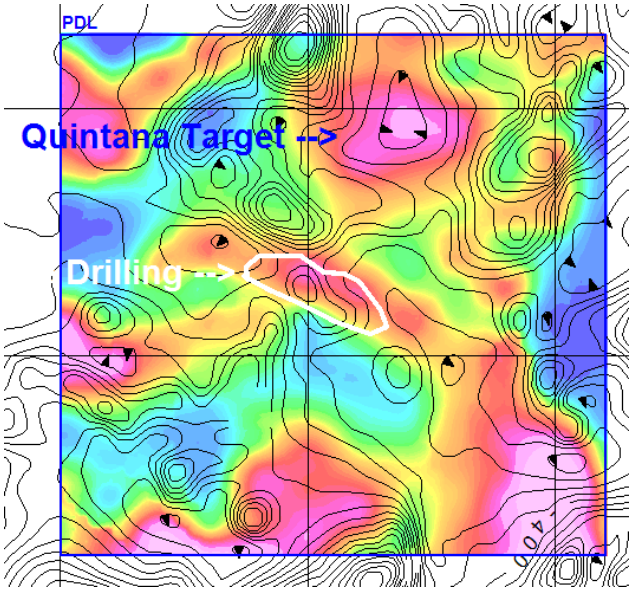

3. Regal Zone

The Regal zone consists of a blanket of chaotic mineralized intrusive blocks with attractive Cu grades, interpreted as a landslide deposit. An IP response parallels northing 5484000N, immediately south and up slope from the Regal zone and so is an obvious drill target. The following figure shows contoured and transparent color IP (3D PDR IP model top cells) over geology (Mihalynuk, 2013). The IP response can be tested along a road at about 683075E, 5483965N.

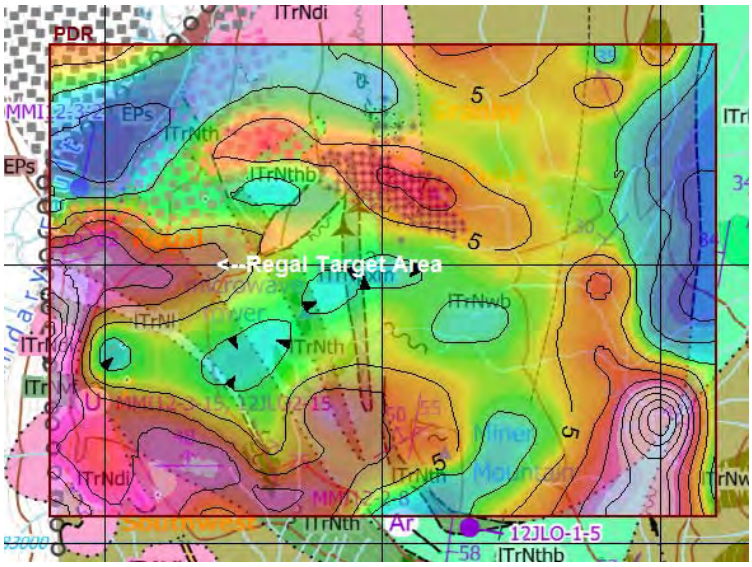

4. Southwest Zone

The Southwest zone of mineralization and alteration, about 1 km south of the Regal zone, coincides with strong IP in the SW corner of the PDR IP inversion model. Two drill holes are within the zone. The IP is open to the south and west. The following figure shows color IP (3D PDR IP model top cells) over contours of RTP mag. The southwest IP highs are located immediately north of strong magnetic anomalies, a situation not unlike that at Copper Mountain. This situation deserves further drill testing. For starters, three recommended drill collar locations are:

682850E, 5483150N – SW corner of IP, on flank of mag anomaly

683350E, 5483300N - bulge in IP response

683800E, 5483400N – IP response and coincident sharp mag anomaly

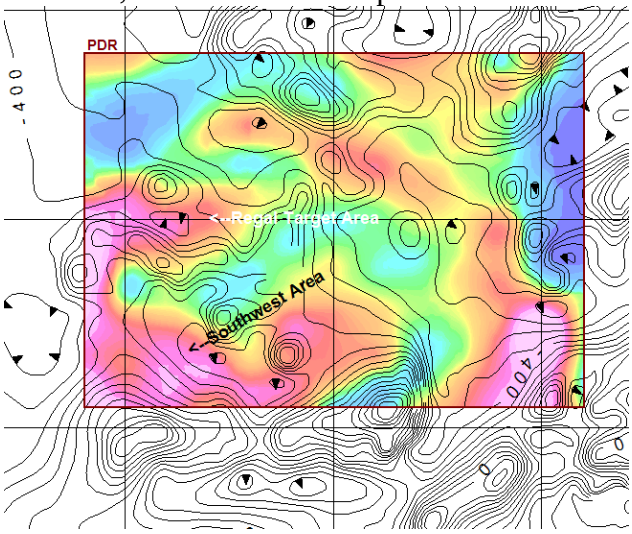

5. Southeast Zone

This a strong shallow IP response near the SE corner of the IP grid at 685000E, 5483500N where it could be tested. A sharp mag low occurs about 100M north. It can be seen in the images of the previous two zones.

6. Deep East Zone

The following sequence of 4 images shows PDL 2D chargeability inversions for the four easternmost lines, using a common color range. They clearly show increasing chargeability at depth to the east, and open further east. There is some suggestion in the 3D inversion models that the Cuba zone plunges down into this deep zone. The shallow Southeast Zone shallow target described above and shown on line 685000E below, appears connected to it at depth. Depth to top for the deep chargeability appears to be in the 100-200M range on the easternmost line, but it could well be shallower further east. Although such a response is not necessarily caused by sulphide mineralization, consideration should be given to testing this large deeper target especially if supported by new geological information.

Line 684600E:

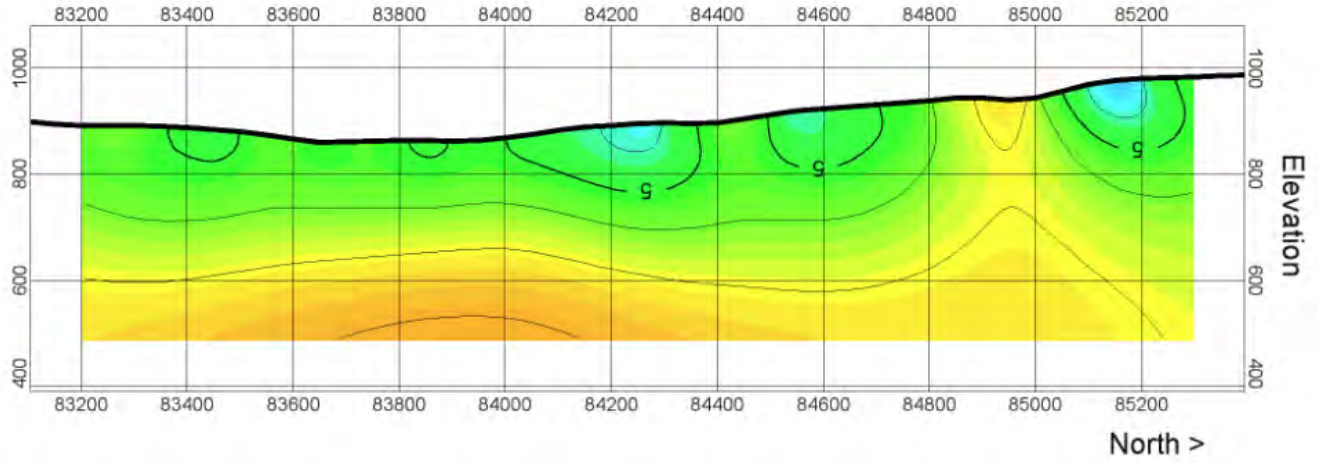

Line 684800E:

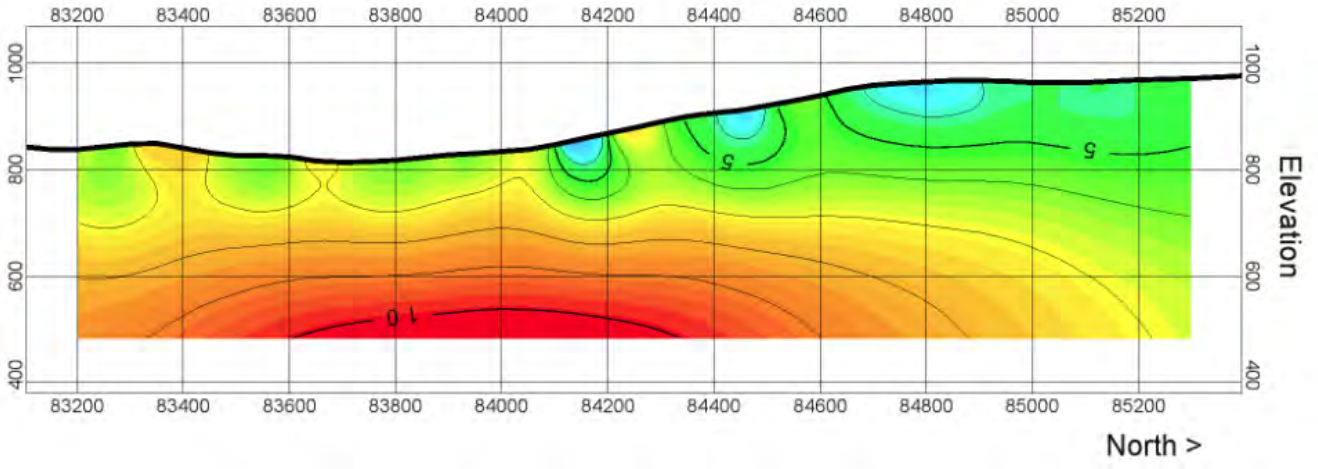

Line 685000E:

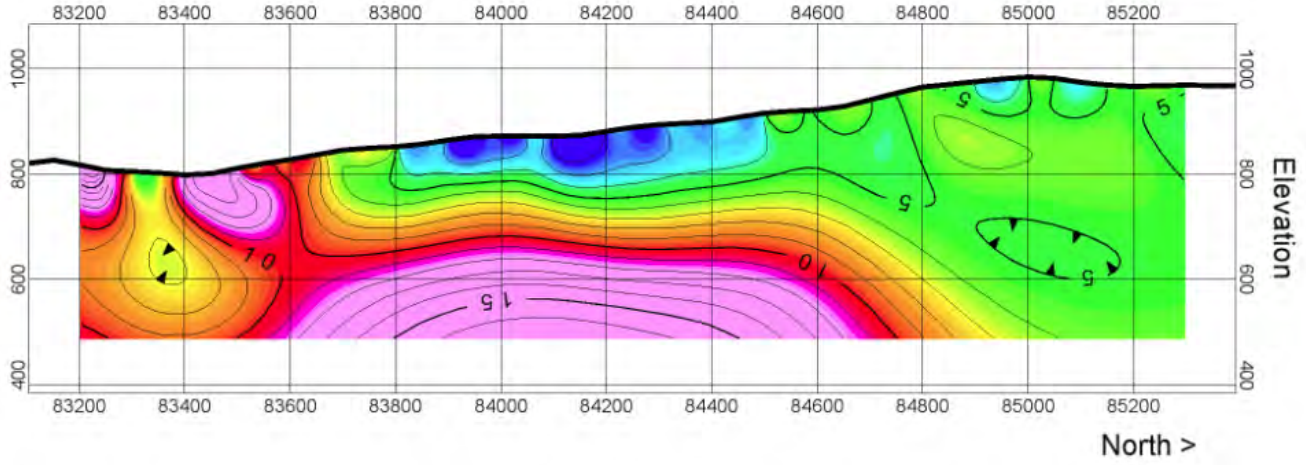

Line 685200E:

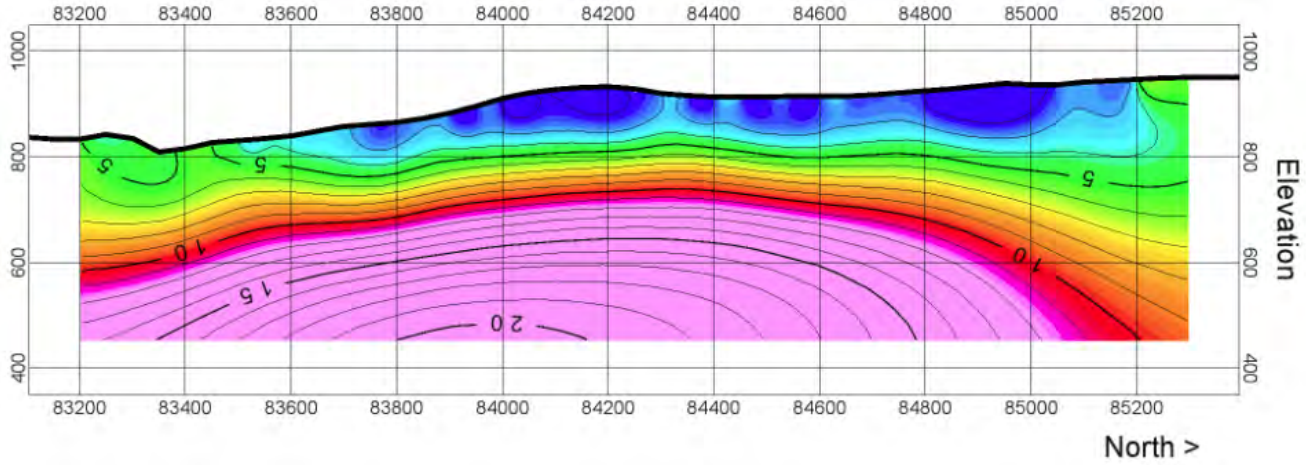

The following target areas are outside the area of IP coverage and based on the results of the Precision Geosurveys airborne data.

7. North Zone

This area is about 1.2 kms north of the Quintana zone. It is characterized by a strong mag low, surrounded by strong mag highs, proximity to the prominent jog in the Boundary Fault on the west side, and a single line K-Th ratio high on the east side of the mag low. Coverage with IP would help define targets. Failing that, a hole collared in the center of the RTP low is at 684250E, 5486125N.
A second hole in this area targeting the K/Th ratio high at the end flank of a magnetic anomaly is at 684350E, 5485975N.

The image below is of the North zone area with RTP color mag and contours of K/Th ratio.

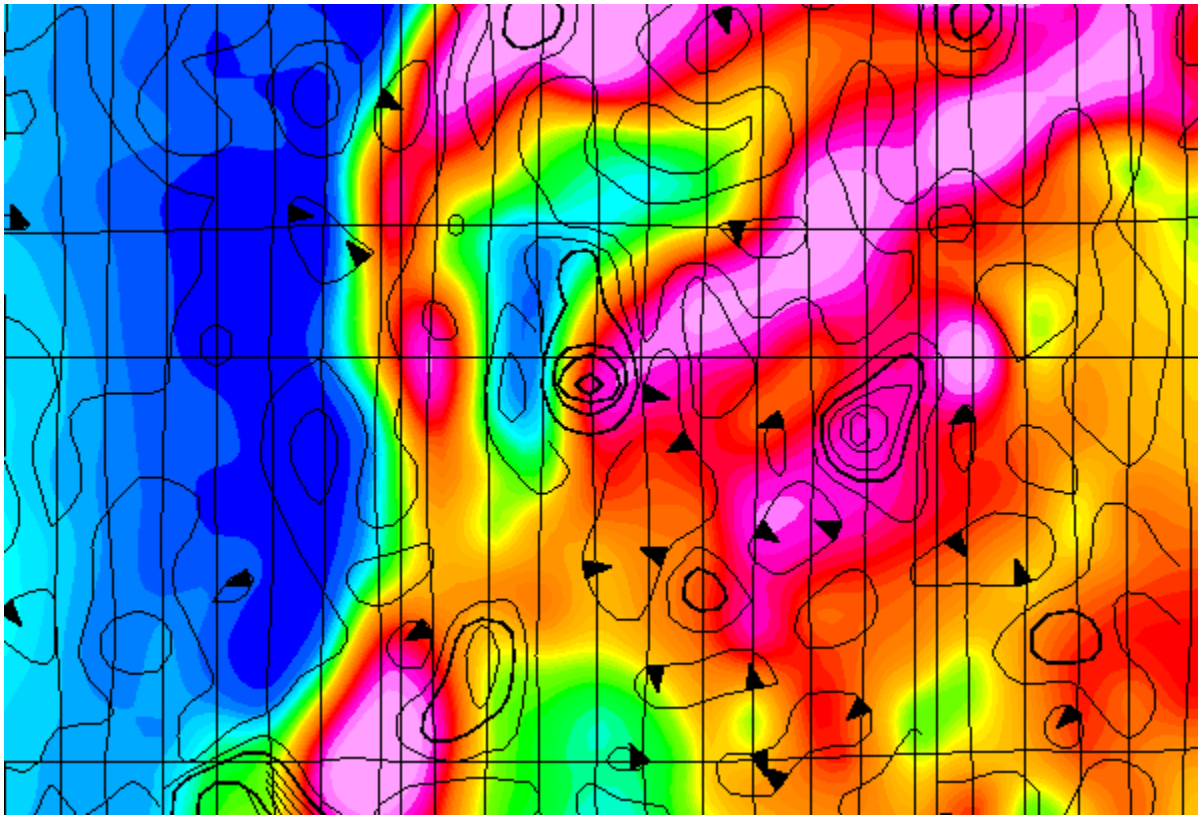

8. North End Zone

This is a large area at the NE end of the survey area. It is characterized by a sub circular area about 1 km in diameter, possibly cut off by the NE striking Boundary Fault, displaying unusually quiet mag (magnetite destruction?), with the center showing somewhat elevated mag and K/Th ratio, as one might expect for the central core of a porphyry system. The following two figures show RTP magnetics and K/Th ratio for the area. Flight lines are 100M apart.

This area should be covered by IP. Failing that, a drill hole in the center of this postulated "system" is at:
685460E, 5487900N

RTP

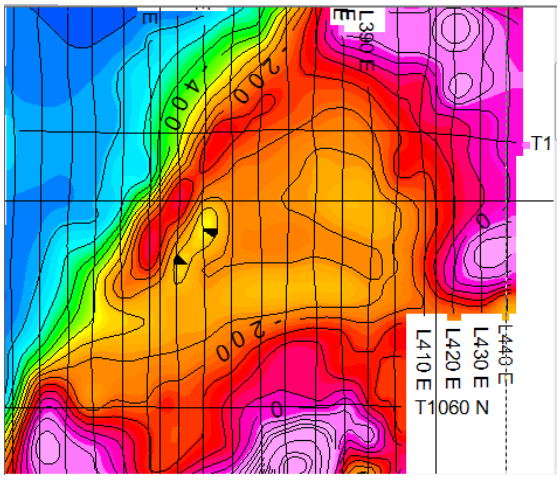

K / Th Ratio

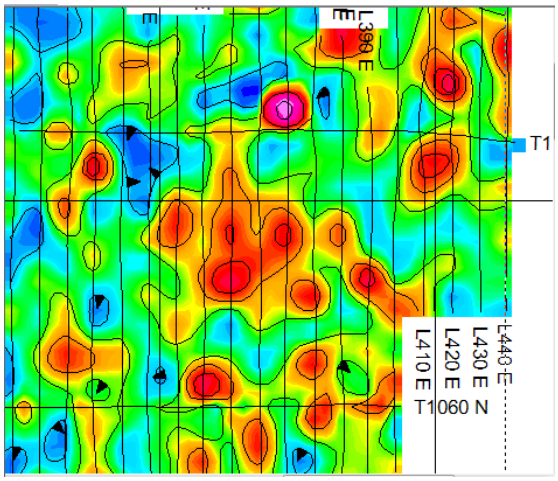

CONCLUSIONS

The Titan 24 IP data have been completely reprocessed producing much smoother geologically believable 2D and 3D (stitched 2D) inversion models. It is expected that this work has added value to the significant expenditure on the Titan IP survey which has produced high quality IP data. Extra map products have been generated from the Precision Geosurveys Inc. aeromag and radiometric data. These combined datasets support high prospectivity for alkalic Cu-Au deposits on the Miner Mountain property.

Six target areas within the IP survey are recommended for drill testing. As well, two areas to the north of the IP survey area have favorable magnetic and radiometric characteristics, and are recommended for IP follow up, or failing that drill testing.

Deposit signatures in the geophysical data could be subtle. It is recommended to continually tie in new geological information from drilling and mapping to the geophysical data for extrapolation purposes.

It is recommended that any further IP on the property consist of standard pole dipole time domain IP using electrode separation of 100M and separations of at least 1 to 6. To calibrate the time domain IP with the Titan phase measurements, a portion of a Titan survey line displaying a range of IP amplitudes should be re surveyed, re-establishing the same stations.

It is recommended to collect core and surface samples when available (there is little outcrop and current drilling is percussion), to submit for physical property measurements to better understand and interpret the geophysical data.

Report by

_____

Jules J. Lajoie, PhD, PEng, FEC
Comtek Enterprises Ltd.
Vancouver BC
June 2013.

REFERENCES

Mihalynuk, M.G., and Logan, J.M., 2013. Geological setting of Late Triassic porphyry Cu-Au mineralization at Miner Mountain, southern British Columbia. BC Geological Survey Paper 2013-1, pp 81-96.

Gharibi, M., and Hearst, R., 2009. Quantec Titan 24 Distributed Acquisition System DC Resistivity & Induced Polarization Surveys, Miner Mountain Project, Princeton, BC, on behalf of Sego Resources Inc. Quantec report for Sego Resources, July 2009.

Poon, J., 2013. Airborne Geophysical Survey Report – Miner Mountain Project. Precision GeoSurveys Inc. report for Sego Resources Inc., June, 2013.

Stanley, C.R., Holbek, P.M., Huyck, H.L.O., Lang, J.R., Preto, V.A.G., Blower, S.J., and Bottaro, J.C., 1995. Geology of the Copper Mountain alkalic copper-gold porphyry deposits, Princeton, British Columbia. In Porphyry Deposits of the Northwestern Cordillera of North America, ed. T.G. Schroeter, CIM Special Volume 46, 1995.